2013-06

Theoretical and experimental study of the excitonic binding energy in GaAs/AlGaAs single and coupled double quantum wells

Journal of Luminescence 144 (2013) 98–104

Contents lists available at SciVerse ScienceDirect

Journal of Luminescence

journal homepage: www.elsevier.com/locate/jlumin

Theoretical and experimental study of the excitonic binding energy in GaAs/AlGaAs single and coupled double quantum wells

E.M. Lopes [a,*,1], D.F. César [b], F. Franchello [c], J.L. Duarte [c], I.F.L. Dias [c], E. Laureto [c], D.C. Elias [d], M.V.M. Pereira [d], P.S.S. Guimarães [d], A.A. Quivy [e]

[a] Departamento de Física, Química e Biologia, Universidade Estadual Paulista, C. P. 266, Presidente Prudente, São Paulo 17700-000, Brazil
[b] Departamento de Física, Universidade Federal de São Carlos, C. P. 676, São Carlos, São Paulo, Brazil
[c] Departamento de Física, Universidade Estadual de Londrina, C. P. 6001, Londrina, Paraná, Brazil
[d] Departamento de Física, Instituto de Ciências Exatas, Universidade Federal de Minas Gerais, C. P. 702, Belo Horizonte, Minas Gerais, Brazil
[e] Laboratório de Novos Materiais Semicondutores, Instituto de Física, Universidade de São Paulo, C. P. 66318, São Paulo, Brazil

ARTICLE INFO

Article history:
Received 12 March 2013
Received in revised form
8 June 2013
Accepted 27 June 2013
Available online 4 July 2013

Keywords:
Excitonic binding energy
Coupled double quantum wells
GaAs/AlGaAs
Magnetophotoluminescence

ABSTRACT

This paper discusses the theoretical and experimental results obtained for the excitonic binding energy (E_b) in a set of single and coupled double quantum wells (SQWs and CDQWs) of GaAs/AlGaAs with different Al concentrations (Al%) and inter-well barrier thicknesses. To obtain the theoretical E_b the method proposed by Mathieu, Lefebvre and Christol (MLC) was used, which is based on the idea of fractional-dimension space, together with the approach proposed by Zhao et al., which extends the MLC method for application in CDQWs. Through magnetophotoluminescence (MPL) measurements performed at 4 K with magnetic fields ranging from 0 T to 12 T, the diamagnetic shift curves were plotted and adjusted using two expressions: one appropriate to fit the curve in the range of low intensity fields and another for the range of high intensity fields, providing the experimental E_b values. The effects of increasing the Al% and the inter-well barrier thickness on E_b are discussed. The E_b reduction when going from the SQW to the CDQW with 5 Å inter-well barrier is clearly observed experimentally for 35% Al concentration and this trend can be noticed even for concentrations as low as 25% and 15%, although the E_b variations in these latter cases are within the error bars. As the Zhao's approach is unable to describe this effect, the wave functions and the probability densities for electrons and holes were calculated, allowing us to explain this effect as being due to a decrease in the spatial superposition of the wave functions caused by the thin inter-well barrier.

1. Introduction

Systems based on semiconductor heterostructures have been widely used for the manufacture of electronic and opto-electronic devices. In this context, coupled double quantum wells (CDQWs) have received considerable attention due to their potential application in opto-electronic devices [1–5] and their importance for academic research, especially on the observation and understanding of new physical effects, such as, for example, the exciton condensation at low temperatures [6–9].

The exciton behavior in heterostructures such as single quantum wells (SQWs) and CDQWs is of great importance for the understanding of their opto-electronic properties. The hydrogen atom model, which is generally used as a basic model to study the exciton dynamics in semiconductor materials, does not provide good results in these systems due to the anisotropy caused by the carriers confinement along the growth direction of the heterostructures. In this scenario, He [10] developed a model known as the fractional-dimension space model, which is able to provide a good description of excitons in low dimensional systems. This model considers the exciton as a hydrogen atom, but in a fractional-dimension space.

Based on the He model, Mathieu, Lefebvre and Christol [11] developed an analytical method known in the literature as MLC method, which provides the effective dimensionality and the excitonic binding energy (E_b) in SQW systems.

Using the work of Mathieu et al., Zhao et al. [12] extended the MLC method for CDQWs and obtained good agreement with experimental results.

A semi-empirical way of estimating the dimensionality of a system and hence E_b is carrying out experiments under applied magnetic fields. A characteristic feature of the application of a magnetic field perpendicular to the layers of a semiconductor

* Corresponding author. Tel.: +55 18 3528 2829.
E-mail address: eldermantovani@yahoo.com.br (E.M. Lopes).
[1] Postal address: Rua Oito, no. 275 – Park Santa Mônica, Osvaldo Cruz, SP, CEP 17700-000, Brazil

0022-2313/$ - see front matter © 2013 Elsevier B.V. All rights reserved.
http://dx.doi.org/10.1016/j.jlumin.2013.06.037

heterostructure is the shift of the energy levels to higher energies, known as diamagnetic shift [13–15]. This diamagnetic shift is directly related to the system dimensionality (and to E_b): the higher the dimensionality the higher is the diamagnetic shift [14,15].

In practice, the diamagnetic shift can be described by distinct expressions for low and high intensity fields. For low fields, the Coulomb potential is much more intense than the magnetic potential and thus E_b is much stronger than the cyclotron energy of the carriers. For intense fields the opposite occurs. Thus, the boundary between the two regimes depends on the E_b magnitude in each system, and hence of their dimensionality. In the case of experiments involving magnetic fields covering both types of behavior the expressions for low and high intensity fields should be used simultaneously to describe the whole diamagnetic shift.

The objective of this study is to determine the behavior of E_b as a function of barrier height (Al concentration—Al%) and inter-well barrier thickness in a set of samples containing GaAs/AlGaAs SQWs and CDQWs and perform a comparative discussion between theoretical and experimental results for these systems. The experimental results were obtained by fitting the diamagnetic shift curves using the appropriated expressions for low and high magnetic field intensities. These curves were constructed from magnetophotoluminescence (MPL) measurements performed at 4 K with varying magnetic field. To obtain the theoretical results, we have used the MLC model combined with the approach proposed by Zhao et al. (in CDQWs cases). The effects of the Al% and, especially, of the inter-well barrier thickness on E_b are discussed.

2. Experimental details

The set of samples used in this study is composed by 6 samples, each one with two different structures made of GaAs wells and AlGaAs barriers. For each sample type shown in Fig. 1, three samples were grown with different Al% at the barriers. So, for a specific structure we can study the influence of the Al% and for a fixed Al% we can investigate the influence of the central barrier thickness.

The samples were grown by molecular beam epitaxy (MBE) on GaAs substrates. First, a 5000 Å thick GaAs buffer layer was grown. Then, a 1000 Å thick AlGaAs layer was grown. Next, for type 1 sample, a 80 Å thick GaAs SQW, a 300 Å thick AlGaAs barrier and a GaAs/AlGaAs CDQW were grown. The CDQW is constituted by two 40 Å thick GaAs quantum wells separated by a 15 Å thick AlGaAs central barrier. For type 2 sample, two GaAs/AlGaAs CDQWs and a 300 Å thick AlGaAs barrier, between the CDQWs, were grown. The first CDQW is constituted by two 40 Å thick GaAs quantum wells separated by a 5 Å thick AlGaAs central barrier while the second one is constituted by two 40 Å thick GaAs quantum wells separated by a 30 Å thick AlGaAs central barrier. Finally, for each sample, there is a 300 Å thick AlGaAs barrier and a 50 Å thick GaAs cap layer. For each sample type we have three samples with different Al%: 15%, 25% and 35%, in a total of 6 samples. Table 1 shows the type and the Al concentration of each sample specifically.

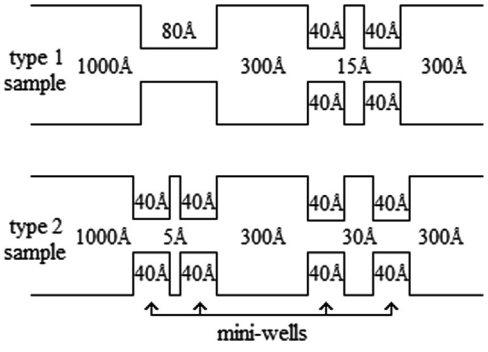

Fig. 1. Schematic potentials for the two types of GaAs/AlGaAs samples: type 1 sample has a 80 Å thick SQW and a CDQW with 40 Å thick mini-wells separated by a 15 Å thick central barrier; type 2 sample has two CDQWs with 40 Å thick mini-wells and different central barriers thicknesses: 5 Å and 30 Å.

MPL measurements were performed at magnetic fields ranging from 0 T to 12 T at 4 K with the magnetic field applied perpendicular to the heterointerfaces. The MPL spectra were detected by using a system combining a 0.75 m single grating spectrometer and a liquid-nitrogen-cooled CCD with an exposure time of 0.4 s. The excitation source was a 5145 Å line of an Ar^+ laser. The excitation light was transmitted to the sample by an optical fiber with a diameter of 400 μm, while the photoluminescence (PL) from the sample to the spectrometer was transmitted by four optical fibers with a diameter of 100 μm. The typical power density of excitation light at the surface of the samples was about 2.6 W/cm^2.

3. Theory

3.1. MLC approach for single and coupled double quantum wells

Considering the exciton as a system of opposite charges interacting via Coulomb potential, their self-energies and orbital radius in volumetric isotropic materials are obtained by solving the Schrödinger equation for the hydrogen atom problem. For the ground state they are given, respectively, by Ref. [10]:

$$E_0 = -\frac{\mu}{m_0\varepsilon^2}E_H \tag{1}$$

$$a_0 = \frac{m_0\varepsilon}{\mu}a_H \tag{2}$$

where μ is the effective reduced mass of the exciton, m_0 is the free-electron mass, ε is the media permittivity, E_H is the Rydberg and a_H is the Bohr radius.

In SQWs and CDQWs the spatial confinement of carriers makes the system anisotropic, making difficult the determination of E_0 and a_0. However, using the fractional-dimension space formalism [10] it is possible to overcome the difficulties caused by confinement and treat the system as isotropic again, but in a space of fractional-dimension α.

Within this approach the excitonic binding energy and the excitonic radius for the ground level are given, respectively, by Ref. [10]:

$$E_b = \left(\frac{2}{\alpha-1}\right)^2 E_0 \tag{3}$$

$$a_b = \left(\frac{\alpha-1}{2}\right)^2 a_0 \tag{4}$$

where α is the dimension, or anisotropy degree, of the system. In SQWs α, which can take continuous values between 2 and 3, can

Table 1
Type and Al concentration of each sample.

Sample	Type	Al (%)
#04	1	35
#05	2	35
#06	1	25
#07	2	25
#08	1	15
#09	2	15

be expressed by Ref. [11]:

$$\alpha = 3 - \exp\left(-\frac{L_w^*}{2a_0}\right) \tag{5}$$

where L_w^* is the effective quantum well width, given by

$$L_w^* = \frac{1}{K_b} + L_w + \frac{1}{K_b} \tag{6}$$

where L_w is the quantum well width and K_b is the characteristic wave vector [11]:

$$\frac{1}{K_b} = \frac{1}{\kappa_{be}} + \frac{1}{\kappa_{bh}} \tag{7}$$

where κ_{be} and κ_{bh} are, respectively, the electron and hole wave vectors at the barriers, given by

$$\kappa_{be(h)} = \frac{1}{\hbar}\sqrt{2m^*_{be(h)}(V_{e(h)} - E_{e(h)})} \tag{8}$$

where $m^*_{be(h)}$, $V_{e(h)}$ *e* $E_{e(h)}$ are, respectively, the mass at the barrier region, the confinement potential and the carrier energy level. L_w^* comprises all the spatial region of carriers interaction, i.e., beyond the well region it also takes into account the carriers wave functions penetration at the potential barriers region.

In order to calculate E_b in CDQWs, Zhao et al. [12] proposed a model that approximates a CDQW to a SQW of effective width $L^*_{w.eff}$. In this model α has the same form showed in Eq. (5); however L_w^* is now given by the following expression:

$$L_w^* = \frac{1}{K_b} + L^*_{w.eff} + \frac{1}{K_b} \tag{9}$$

where $L^*_{w.eff}$ is given by

$$L^*_{w.eff} = L_{w1} + L_{w2}e^{-L_bK_b} \tag{10}$$

where L_{w1} and L_{w2} are the mini-wells thicknesses, L_b is the inter-well barrier thickness and K_b is the characteristic wave vector of the carriers penetration into the inter-well barrier, and has a form similar to that shown in Eq. (7).

3.2. Excitons in magnetic fields

In the presence of an external magnetic field the electron–hole pair interacts through an effective potential, comprising the Coulomb term, corresponding to the binding energy of the pair, and the magnetic interaction term, corresponding to the cyclotron energy ($\hbar\omega_c/2$, where ω_c is the carrier's cyclotron frequency). In this scenario, the exciton self-energies will be determined by the intensity of the applied magnetic field.

For low intensity fields ($\hbar\omega_c/2 << E_b$) the excitonic binding energy, now called E_B(B), is mainly determined by the Coulomb term. Thus, the potential due to the magnetic field becomes only a perturbation and E_B(B) can be expressed as:

$$E_B(B) = \Delta E(B) - \left|E_b(0)\right| \tag{11}$$

where $\Delta E(B)$, the diamagnetic shift, is the contribution due to the magnetic field and E_b is the contribution due to the Coulomb potential. Using perturbation theory one can show that $\Delta E(B)$ is given by Ref. [16]:

$$\Delta E(B) = D_1\frac{\varepsilon_0^2\varepsilon_r^2h^4}{4\pi^2e^2\mu^3}B^2 \tag{12}$$

where $\varepsilon_0\varepsilon_r$ is the media permittivity, e is the electronic charge, μ is the reduced effective mass and B is the magnitude of the applied magnetic field. D_1 describes the system dimensionality and takes values between 3/16 (2D) and 1 (3D).

In magnetic fields for which the cyclotron energy is of the order of the Coulomb energy ($\hbar\omega_c/2 \approx E_b$) the system configuration changes and is no longer possible to use perturbation theory. In this case $E_B(B)$ can be expressed by Ref. [16]:

$$E_B(B) \approx 3D_2\left[\frac{\hbar eR_{ex}B}{2(2n_l+1)\mu}\right]^{1/2} \tag{13}$$

where R_{ex} is the effective Rydberg constant of a 3D exciton and D_2 describes the system dimensionality, assuming values between 1 (2D) and 0.25 (3D).

The parameters D_1 *e* D_2 are directly related to the system dimensionality α. The relation between D_1 and α is obtained through perturbation theory, but within the formalism of the fractional-dimension space, and is given by Ref. [14]:

$$D_1 = \frac{3(\alpha-1)^4}{2^{\alpha+1}\alpha} \tag{14}$$

D_2 can be connected to E_b at null magnetic field ((Eq. (3)):

$$E_b(0) = -4D_2R_{ex} \tag{15}$$

Then, taking the limits for D_2, $E_b(0)$ can vary between $-4R_{ex} \leq E_b(0) \leq -R_{ex}$. Comparing Eqs. (3) and (15) (for $n=1$) one has:

$$D_2 = \left(\frac{1}{\alpha-1}\right)^2 \tag{16}$$

Therefore the equations that describe the diamagnetic shift can be expressed as:

$$\Delta E_1(B) = \frac{3(\alpha-1)^4}{2^{\alpha+1}\alpha}\frac{\varepsilon_0^2\varepsilon^2h^4}{4\pi^2e^2\mu^3}B^2 \tag{17}$$

for low intensity fields and

$$\Delta E_2 = \frac{\hbar e}{2\mu}B - \left|\frac{3}{(\alpha-1)^2}\left(\frac{\hbar e}{2\mu}R_{ex}\right)^{1/2}\right|B^{1/2} \tag{18}$$

in the high magnetic field limit.

Eqs. (17) and (18) will be used to fit the experimental results for the diamagnetic shifts obtained through MPL measurements.

4. Experimental results

Fig. 2 shows, as examples, the MPL spectra obtained for samples #04, #07 *e* #09 at 4 K and different magnetic fields. The spectra obtained for the other samples, except sample #05, exhibit similar behavior to those shown in this figure. In order to confirm the origin of the transitions, the energy levels of electrons (e), heavy holes (hh) and light holes (lh) were calculated [17]. The energy difference between the hh and lh energy levels shows that at the temperature the PL spectra were obtained (4 K) only the hh levels are populated. Therefore, the results allow to attribute unambiguously the observed PL peaks as being due to transitions related to the first symmetric electron level and the first symmetric heavy hole level in the CDQWs.

Fig. 3 shows exclusively the MPL spectra obtained for sample # 05. Unlike the well-defined PL peaks, as those obtained for all other samples, in these spectra two wider PL bands are observed, each one consisting of two recombination channels. The split of the PL bands is due to the existence of bimodal heterointerface roughness in the CDQWs. The details of the results obtained for this sample are discussed in two specific works previously published [18,19].

The experimental determination of the dimensionality, the effective mass of carriers and the excitonic binding energy is

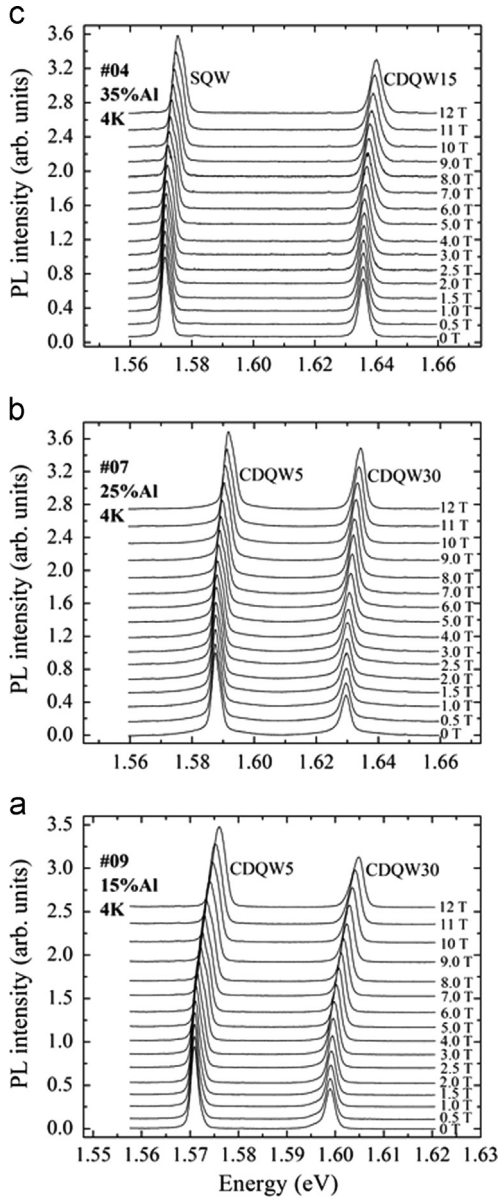

Fig. 2. MPL spectra at magnetic fields ranging from 0 T to 12 T for three samples: (a) #09, (b) #07, and (c) #04.

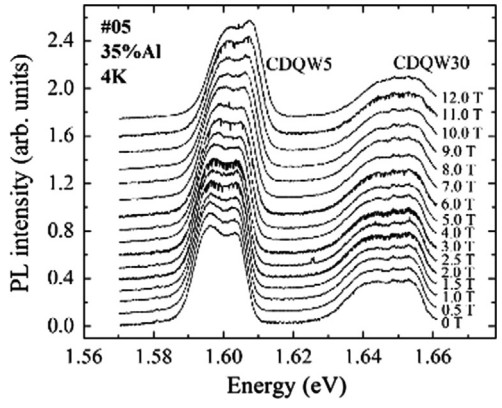

Fig. 3. MPL spectra at magnetic fields ranging from 0 T to 12 T for sample #05.

done by fitting the diamagnetic shift curves. These curves can be constructed from the PL peak energy of each sample, considering how much this energy is shifted for a given magnetic field in relation to the emission at null field. For the sake of illustrating, Fig. 4 shows these experimental curves (solid circles) and the fits (lines) obtained for some heterostructures of the studied samples (the results obtained for the other heterostructures are similar).

The fitting of the experimental curves is done by using the expressions for low and high intensity magnetic fields, Eqs. (17) and (18), respectively, on the same graphic. Eqs. (17) and (18) have common values of α and μ and so the fitting procedure must be performed simultaneously, with the same values for α and μ in both equations. Thus, for each heterostructure is possible to determine a set of parameters α and μ that is common to both regimes simultaneously. With these values is possible to determine E_b from Eq. (3).

5. Discussion

5.1. Theoretical vs. experimental results

Table 2 shows the comparison between the theoretical values obtained by the MLC method in conjunction with the approximation suggested by Zhao et al. and the experimental results for dimensionality and effective mass obtained for all heterostructures. For CDQW5 with 35% Al it was considered the fit for the higher energy channel observed at the PL band, while for CDQW30 with the same Al concentration it was considered the fit for the lower energy channel (these two channels are related to the structural configuration which best represents the nominal dimensions of the mini-wells in each CDQW [18]).

In general, the theoretical results show good agreement with the experimental ones. The system dimensionality α shows the expected behavior: for the SQW α reaches the highest value and for the CDQW30 α is minimum. This was expected since the introduction of the inter-well barrier and its thickening increases the confinement of the carriers, until the inter-well barriers are so thick that the mini-wells become decoupled.

Regarding the effective mass, although the absolute results show good agreement, the behavior predicted theoretically is opposite to the experimental one (different behavior is also observed for the Al concentration of 35%). However, the analysis of the effective mass is complex and depends on several factors, such as, for example: the wave function penetration at the barriers, the nonparabolicity of the conduction band, the mismatch of the conduction band between well and barriers and α itself. Furthermore, the fluctuation on the effective mass values is small and it is within the error associated to the diamagnetic shift data. In the following analysis we will restrict the discussion to E_b results.

Table 3 shows the comparison between the theoretical and the experimental results obtained for E_b in all heterostructures.

The experimental and theoretical results presented in Table 3 show good agreement with each other. In general E_b and α have an inverse behavior, which was expected since the higher the system dimensionality the smaller the carriers confinement and the lower is E_b. For CDQW5 the experimental binding energy is slightly lower than that for the SQW. This interesting effect will be discussed in the next section.

In order to illustrate the overall result, the dependence of the optical transition energy as a function of inter-well thickness is shown in Fig. 5 for all heterostructures. The theoretical values were obtained from calculations based on the envelope function formalism [17] and considering the theoretical results for E_b. The experimental values were extracted directly from the MPL spectra obtained at low temperature and zero magnetic field. There is a good agreement between theory and experiment.

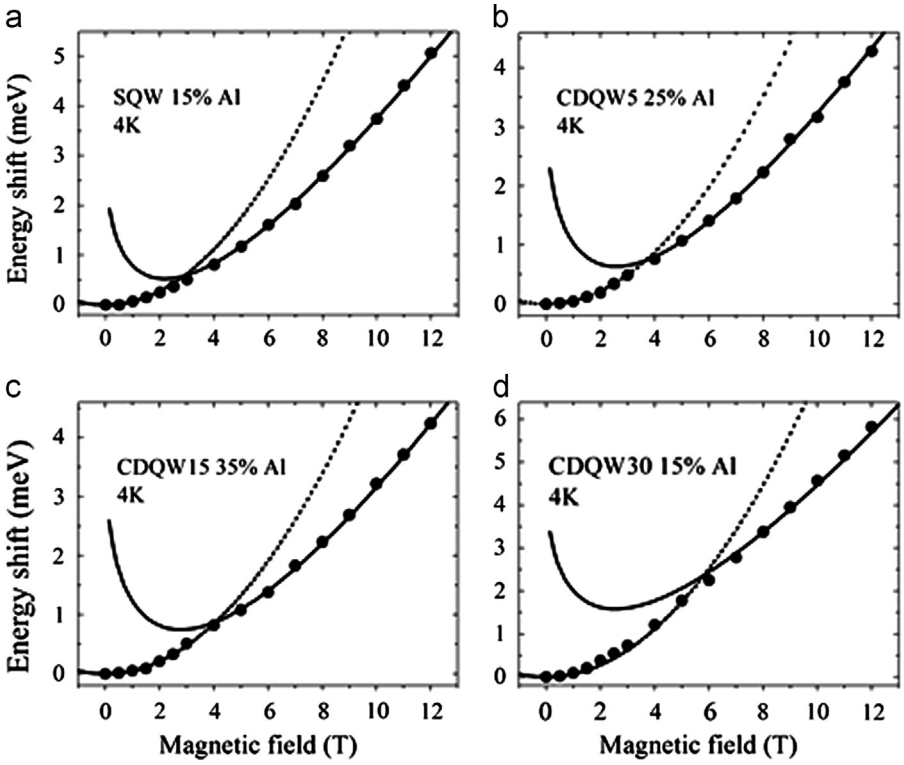

Fig. 4. Diamagnetic shift experimental curves and the respective fits for some heterostructures. The experimental data are represented by the solid circles while the fits for low and high magnetic fields are represented by the dashed and continuous lines, respectively.

Table 2
Theoretical and experimental results obtained for μ and α for all the heterostructures.

Heterostructure	μ^*_{th}	μ^*_{exp}	α_{th}	α_{ex}
15% Al				
SQW	0.049	0.051	2.44	2.45
CDQW5	0.050	0.050	2.44	2.44
CDQW15	0.050	0.049	2.43	2.41
CDQW30	0.050	0.049	2.42	2.38
25% Al				
SQW	0.051	0.055	2.41	2.42
CDQW5	0.052	0.054	2.40	2.41
CDQW15	0.053	0.052	2.39	2.38
CDQW30	0.054	0.052	2.37	2.35
35% Al				
SQW	0.053	0.055	2.40	2.40
CDQW5	0.055	0.050	2.38	2.38
CDQW15	0.056	0.054	2.37	2.38
CDQW30	0.057	0.056	2.34	2.35

Table 3
Theoretical and experimental results obtained for E_b for all the heterostructures.

Heterostructure	$E_{b(th)}$(meV)	$E_{b(exp)}$(meV)
15% Al		
SQW	8.78	8.60
CDQW5	8.90	8.57
CDQW15	9.10	8.78
CDQW30	9.31	9.19
25% Al		
SQW	9.81	9.73
CDQW5	10.11	9.71
CDQW15	10.56	9.81
CDQW30	11.03	10.34
35% Al		
SQW	10.59	10.05
CDQW5	11.32	9.44
CDQW15	11.81	10.16
CDQW30	12.57	11.18

5.2. Analysis of the excitonic binding energy E_b

Now, a discussion about the behavior of E_b (experimental results) as a function of the Al% and the inter-well barrier thickness will be presented.

As can be observed in Table 3, for a given heterostructure, the higher the Al% the higher the E_b. This is the expected behavior since an increase in Al% causes an increase in the AlGaAs energy gap, which increases the exciton confinement in the mini-wells region and, consequently, increases E_b.

On the other hand, the behavior of the experimental E_b as a function of the inter-well barrier thickness, shown in Fig. 6, presents an interesting characteristic: for each Al% value, despite the relatively large error associated to the experimental data, E_b tends to reduce when passing from the SQW to CDQW5 and then increases when going to the CDQW15 and CDQW30. Although this effect is not described by the theoretical approach used, it has been already predicted by other authors using more elaborated methods [20,21]. According to Bayer et al. [22] who investigated the effect of inserting AlAs inter-well barriers in $Al_{0.30}Ga_{0.70}As$/GaAs quantum wells, this reduction in E_b can be explained by the fact that between the limiting cases of (i) having an inter-well barrier very thick (corresponding to two independent mini-wells of width L_w) and (ii) having no inter-well barrier (corresponding to a single well of width $2L_w$), where the maximum of the electrons and holes wave functions are located at the center of the single well, narrow inter-well barriers cause smaller overlap of the carriers wave functions due to the difference between the masses of these particles (the electron wave functions are less disturbed by the inter-well barrier) and thus the Coulomb interaction between electrons and holes is lower and, consequently, E_b decreases.

Bayer et al. [22] observed the effect of reducing E_b for AlAs inter-well barriers. Our results show that in CDQWs with 5 Å thick $Al_xGa_{1-x}As$ inter-well barriers the reduction also occurs and is clearly observed for 35% Al concentration and this trend can be noticed for concentrations as low as 15%, although for this latter case the E_b decrease is within the error bar. In the case observed in this work, the effect is similar to that discussed above when introducing the AlAs inter-well barrier: for the 5 Å inter-well barrier the heavy hole wave function undergoes a greater change, in comparison to the heavy hole wave function at the 80 Å SQW, than the change experienced by the electron wave function; hence, the superposition of the two wave functions decreases and, consequently, E_b decreases with respect to the SQW excitonic binding energy. This effect is more pronounced as the Al% increases, as shown in Fig. 6.

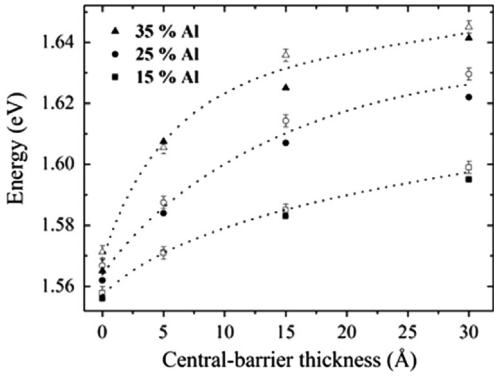

Fig. 5. Theoretical (solid symbols) and experimental (open symbols) dependence of the optical transition energy as a function of central barrier thickness for all the heterostructures. For the CDQW5 and CDQW30 with 35% Al the data from the higher energy and lower energy channels, respectively, were considered. The dotted lines are guides for the eye.

To verify the above argument, we have calculated [23] the normalized probability densities $|\psi|^2$ (PD) for the electronic (e_1) and heavy hole (hh_1) ground levels in the CDQWs with 35% Al, which are presented in Fig. 7. The simplest analysis that provides information about the overlapping of the electron and heavy hole wave functions and, consequently, about E_b, is the comparison of the distance between the positions of maximum PD for electrons and holes in each CDQW. Comparing with the 80 Å SQW (not

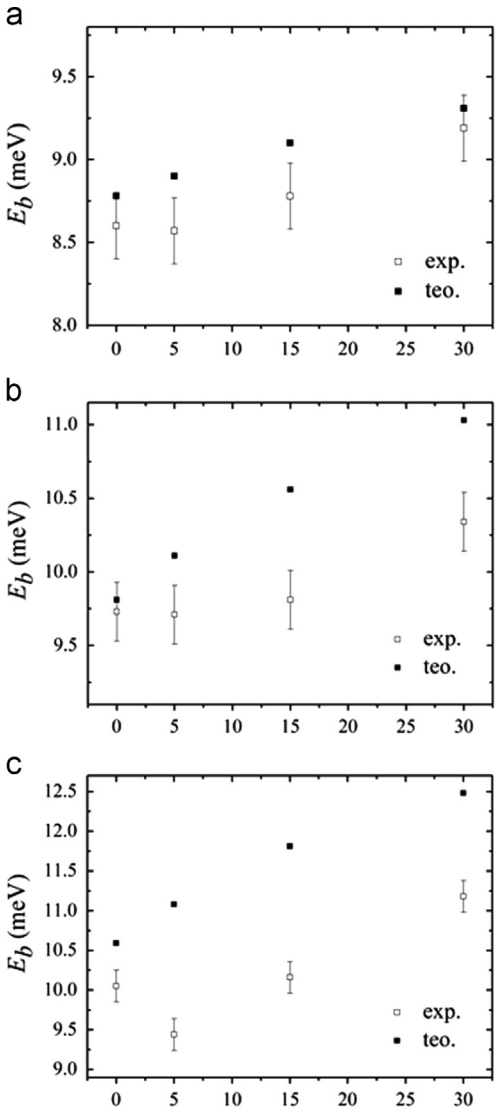

Fig. 6. Theoretical (solid squares) and experimental (open squares) dependence of the excitonic binding energy as a function of central barrier thickness for the three Al concentrations at barriers: (a) 15%; (b) 25% and (c) 35%.

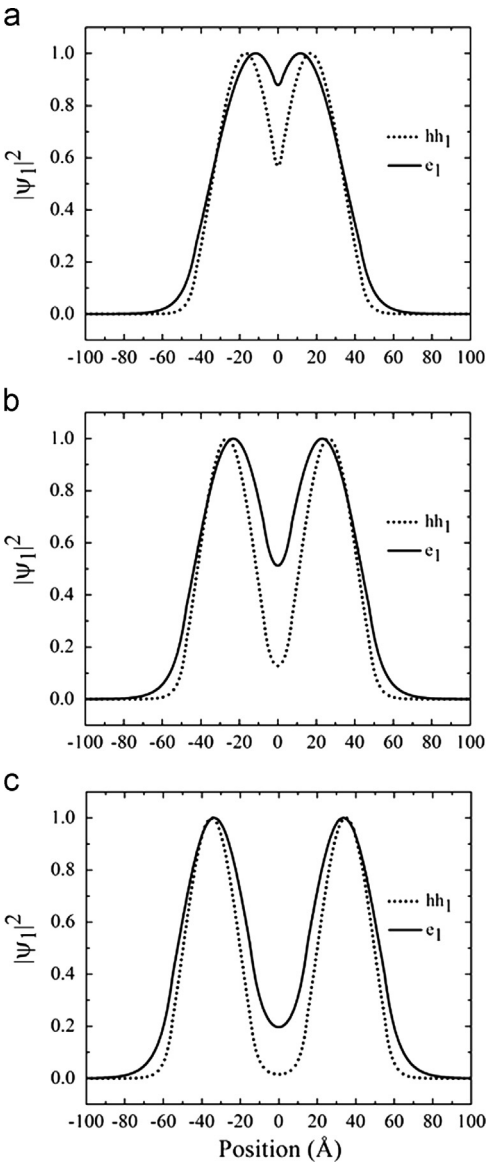

Fig. 7. Normalized square of the electron (solid) and the heavy hole (doted) ground-state wave functions for: (a) CDQW5, (b) CDQW15 and (c) CDQW30 with 35% Al.

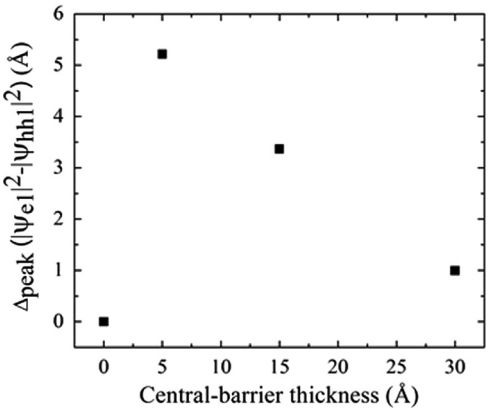

Fig. 8. Distance between the maximum of the square electron and heavy hole ground-state wave functions as a function of central-barrier thickness for the heterostructures with 35% Al.

shown here), where the maximum PD for both electrons and holes is centered at the well, for the CDQW5 the 5 Å inter-well barrier considerably modifies the hole PD but has little effect on electron PD, causing a pronounced separation between the two maxima (Fig. 7a). As the inter-well barrier thickness increases (CDQW15 and CDQW30) the PD maxima come close again, tending to the situation where the two mini-wells are isolated and then the position of PD maxima coincide again. To better visualize the separation between the electrons and holes PD maxima, a graph of this separation as a function of the inter-well barrier is shown in Fig. 8. In this figure one can see that the maximum separation (equivalent to a minimum in E_b) occurs for L_b about 5 Å and, after this, the separation decreases again, as expected.

6. Conclusions

In summary, we have determined the influence of the height and the thickness of the inter-well barrier on the excitonic binding energy (E_b) in GaAs/$Al_xGa_{1-x}As$ CDQWs. Our experimental results were obtained using an alternative approach based on diamagnetic shift curves, constructed from MPL measurements. Initially, the theoretical results were obtained using the MLC model for the fractional-dimension space added to the approach proposed by Zhao et al. for the CDQWs treatment. Our experimental results show that, relative to the SQW, the insertion of a 5 Å inter-well barrier decreases E_b and, with a further barrier increase, E_b increases. This behavior decreases with Al% decrease, being very well defined for 35% Al concentration and can be noticed for an Al % as low as 15%, although in this latter case the E_b variation is within the error bar. The MLC method with the approach proposed by Zhao, although very useful for estimating E_b and for calculating the optical transition energies, is unable to explain the E_b decrease with the introduction of the very narrow inter-well barrier. The calculation of the wave functions and of the probability densities has shown that the E_b behavior is due to a decrease in the spatial superposition of the electron and hole wave functions with the introduction of the thin inter-well barrier, which in turn, is due to the difference in the interaction of each type of carrier with this barrier.

Acknowledgments

The authors would like to acknowledge the financial support granted by the Brazilian agencies Fundação de Amparo à Pesquisa do Estado de São Paulo (FAPESP), Coordenação de Aperfeiçoamento de Pessoal de Nível Superior (CAPES), Conselho Nacional de Desenvolvimento Científico e Tecnológico (CNPq), Fundação Araucária de Apoio ao Desenvolvimento Científico e Tecnológico do Paraná (Fundação Araucária), Fundo de Apoio ao Ensino, à Pesquisa e à Extensão (FAPE-UEL) and Fundação de Amparo à Pesquisa do Estado de Minas Gerais (FAPEMIG). PSSG is supported by INCT-DISSE, Instituto Nacional de Ciência e Tecnologia de Nanodispositivos Semicondutores, Brazil.

References

[1] X.G. Peralta, S.J. Allen, M.C. Wanke, N.E. Harff, J.A. Simmons, M.P. Lilly, J.L. Reno, P.J. Burke, J.P. Eisenstein, Appl. Phys. Lett. 81 (2002) 1627.
[2] X.G.P. Grish, Ph.D. Thesis, University of California, Santa Barbara, 2002.
[3] P. Jänes, P. Holmström, U. Ekenberg, IEEE J. Quantum Electron. 38 (2002) 178.
[4] H. Yoshikda, T. Simoyama, V.A. Gopal, J. Kasai, T. Mozume, H. Ishikawa, IEICE Trans. Electron. E87C (7) (2004) 1134.
[5] M. Miura, S. Katayama, Sci. Technol. Adv. Mater. (2006) 286.
[6] A.V. Larionov, V.E. Bisti, M. Bayer, J. Hvan, K. Soerensen, Phys. Rev. B: Condens. Matter 73 (2006) 235329.
[7] B. Laikhtman, R. Rapaport, Phys. Rev. B: Condens. Matter 80 (2009) 195313.
[8] H.T. Ng, S.I. Chu, Phys. Rev. A: At. Mol. Opt. Phys. 84 (2011) 023629.
[9] G.J. Schinner, E. Schubert, M.P. Stallhofer, J.P. Kotthaus, D. Schuh, A.K. Rai, D. Reuter, A.D. Wieck, A.O. Govorov, Phys. Rev. B: Condens. Matter 83 (2011) 165308.
[10] X.F. He, Phys. Rev. B: Condens. Matter 43 (1991) 2063.
[11] M. Mathieu, P. Lefebvre, P. Christol, Phys. Rev. B: Condens. Matter 46 (1992) 4092.
[12] Q.X. Zhao, B. Monemar, P.O. Holtz, M Willander, B.O. Fimland, K. Johannessen, Phys. Rev. B: Condens. Matter 50 (1994) 4476.
[13] I. Aksenov, J. Kusano, Y. Aoyagi, T. Sugano, T. Yasuda, Y. Segawa, Phys. Rev. B: Condens. Matter 51 (1995) 4278.
[14] A. Thilagam, Physica B 262 (1999) 390.
[15] N. Miura, Y.H. Matsuda, K. Uchida, H. Arimoto, J. Phys. Condens. Matter 11 (1999) 5917.
[16] O. Jaschinski, M. Vergöhl, J. Schoenes, A. Schlachetzki, P. Bönsch, Phys. Rev. B: Condens. Matter 57 (1998) 13086.
[17] G. Bastard, Wave mechanics applied to semiconductor heterostructures, Les Ulis: Les Editions de Physique (1988).
[18] E.M. Lopes, J.L. Duarte, L.C. Poças, I.F.L. Dias, E. Laureto, A.A. Quivy, T.E. Lamas, J. Lumin. 130 (2010) 460.
[19] E.M. Lopes, J.L. Duarte, I.F.L. Dias, E. Laureto, P.S.S. Guimarães, A.G.S. Subtil, A.A. Quivy, J. Lumin. 132 (2012) 11830.
[20] J. Cen, K.K. Bajaj, Phys. Rev. B: Condens. Matter 46 (1992) 15280.
[21] F. Vera, Z. Barticevic, J. Appl. Phys. 83 (1998) 7720.
[22] M. Bayer, V.B. Timofeev, F. Faller, T. Gutbrod, A. Forchel, Phys. Rev. B: Condens. Matter 54 (1996) 8799.
[23] We Used the Software Quantum Well Solver to Calculate $|\psi|^2$: R.Y. Tanaka, A. Passaro, N.M. Abe, J.M. Villas-Boas, G.S. Vieira, S. Stephany, SBMO/IEEE MTT-S International Microwave and Optoelectronics Conference, 2007, pp. 914.